Manuscript

Experimental studies on bubble pump operated diffusion absorption machine based on light hydrocarbons

N. Ben Ezzine[1*], R. Garma[2], M. Bourouis[3], A. Bellagi[4]

[1,2,4]U.R. Thermique et Thermodynamique des Procédés Industriels, Ecole Nationale d'Ingénieurs de Monastir, Av. Ibn Jazzar, 5060 Monastir, Tunisia
[3]Center CREVER, Universitat Rovira i Virgili,
43006 Tarragona, Spain
n_benezzine@yahoo.fr

Abstract

An experimental investigation of an air cooled diffusion-absorption machine operating with binary light hydrocarbon mixtures (C_4H_{10}/C_9H_{20}) as working fluids and helium as pressure equalizing inert gas is presented in this paper. The machine, which is made of copper an available and very good heat conducting metal, is intended to be powered with solar heat from flat plate or common evacuated tube collectors. The cooling capacity is 30-40 W. Cold is produced at temperatures between -10 and +10°C for a driving temperature in the range 120-150°C.

Key words: Diffusion Absorption Refrigeration, experimental investigation, C_4H_{10}/C_9H_{20} working fluids, bubble pump, coefficient of performance

Nomenclature:

COP	coefficient of performance	*Subscripts*	
C_p	specific heat capacity, J/kg°C	B	boiler
m	mass flow rate, $Kg.s^{-1}$	bp	bubble pump
GHX	gas heat exchanger	G	generator
$\dot{Q}$	heat flow, W	CV	control volume
t	time, mn	loss	losses
T	temperature, °C	W	water
U	internal energy		

I. Introduction

The diffusion absorption technique invented by the Swedish engineers von Platen and Munters [1] in the 1920s best suited for solar applications. The corresponding thermodynamic cycle is based on refrigerant/absorbent pair mixture as working fluids and an inert gas for pressure equalization. A thermally driven bubble pump, which can be powered by waste heat or solar thermal energy, is used to lift the liquid solution. As a result of the absence of any mechanical moving part, the refrigerator is silent and very reliable [2] in addition of an economical and natural relative cycle.

The most used working fluid for this called diffusion absorption refrigerator, manufactured and commercialised by Electrolux AB Sweden (today Domestic AB) [3], is the ammonia/water system with ammonia as refrigerant and water as absorbent. To maintain a uniform pressure throughout the machine the hydrogen is used as auxiliary gas in the cold component [4, 5].

Using ammonia/water mixture provides cooling at very low temperature, -20 to -30°C, depending on the diffusion absorption cycle configuration [2, 6], requires therefore high driving temperatures, higher than 150°C, which is incompatible with solar heat. Furthermore, ammonia is corrosive to copper, the material of choice for this kind of equipment.

An alternative working fluid mixture with an alternative technique exists: the lithium bromide/ water system. With this mixture, lower driving heat temperatures (below 100°C) [7] are possible, so also the use of thermal solar energy sources. Nevertheless, it presents some difficulties like to be operated under very low pressures and essentially problems associated with the crystallisation of the salt. Because water is the refrigerant, lower temperatures than 0°C are not possible.

A working fluid which is based on organic fluids (organic solvent in combination with a HFC as refrigerant) was investigated [2, 5] and it is concluded that a complete diffusion refrigerating system that uses this mixture may be powered by solar energy.

It can be noted that the search for alternative working fluids proper to be used with diffusion absorption machine for solar applications continues to be the focus of active research in the field of refrigeration and air conditioning. In this contest, a low capacity diffusion absorption machine operating with a binary light hydrocarbons mixture is designed, constructed and investigated. The present paper reports on the first experimental results.

II. Working principle

Figure 1 shows a simplified schematic diagram of the Platen-Munters diffusion absorption machine composed of a condenser, an evaporator/gas heat exchanger, an absorber, a solution heat exchanger and a generator including a bubble pump and a boiler. The rich solution arriving to the generator is heated up (10) by the heat flux Q_{bp} applied in the bottom of the bubble pump which causes the evaporation of some refrigerant (butane). Small vapor bubbles are first produced which then form plugs filling the whole tube section. The rising bubbles act as small gas pistons lifting liquid slugs to the tube's top (11). The pumped solution gets eventually further heated by an additional heat flux Q_B

provided to the boiler, so an additional quantity of vapor is generated. The resulting poor solution leaves the generator (8) toward the absorber via the solution heat exchanger while the vapor rises toward the condenser through the rectifier (12) where the rest of absorbent nonane vapor is removed by partial condensation. The formed liquid falls back into the boiler (13) and join the weak solution. The purified butane vapor condenses in the condenser releasing condensation heat to the surrounding air. The resulting condensate (2) flows to the evaporator. Uncondensed gas flows to the reservoir (absorber's bottom) through the gas bypass (2'). At the evaporator entrance (4), the partial pressure of the liquid butane is reduced due to mixing with the helium gas returning from the absorber. As a result, the liquid butane begins evaporating. The resulting cold and heavy butane-helium gas mixture leaves the evaporator, falls down in the reservoir (5) and flows upward the absorber in counter current to the weak solution arriving from the absorber's top (9). Along the absorber the weak solution absorbs the butane vapor. The residual helium-butane gas mixture (3) flows upward to the evaporator and the rich solution at the bottom flows down toward the generator (7) via the solution heat exchanger where it is pre-heated.

III. Experimental set up and procedure

For the purposes of the present study, an experimental prototype was built in order to investigate the performance of a bubble pump operated diffusion absorption refrigerator based on light hydrocarbons. The machine is made of copper. Its nominal cooling capacity is 30-50 W.

The working fluids mixture is composed of n-butane as refrigerant, n-nonane as absorbent and helium as pressure equalizing inert gas.

III.1. Experimental set up

A schematic assembly diagram of the experimental set up is given in figure 2. The system design allows investigating the bubble pump behaviour and the absorber efficiency.

The design of the main components is as follows:

Generator

As shown in figure 2, the boiler and the bubble pump are not combined in one unit as is a classical DAR but separated in order to investigate each of both machine components independently from one another. Therefore the generator consists of:

- a single vertical tube (height: 800 mm, diameter: 8/10 mm) to which the heat input is restricted to a small zone in the bottom,
- a vapor-liquid separator connected to the tube and
- a boiler.

Condenser

As the machine is intended to be powered with thermal solar heat the condenser is air-cooled. 58x3 fins enhance the heat transfer process (Fig. 3).

Absorber

For the same raison, the absorber is also air-cooled. It is constituted of a folded tube (700x21 mm in length and 18/20 mm in diameter) which forms two planes with a variable angle between them. The absorber efficiency is a function of the residence times of the gas and the liquid which themselves depend on the opening between the planes. Figure 4 shows the absorber design.

Evaporator-gas heat exchanger

As illustrated in figure 2, the evaporator/gas heat exchanger is a shell and tube HX, to which the condensate refrigerant tube is attached in order to provide some sub-cooling of the liquid refrigerant before it gets in the evaporator.

III.2. Procedure

First, the whole machine is evacuated using a rotary vacuum pump. The reservoir is thereafter charged with liquid n-nonane followed by butane vapor. Finally, helium (inert gas) is added until the required total pressure is reached.

Fifteen calibrated K-type thermocouples are used to measure the temperatures at different locations of the apparatus. The temperatures are loaded and stored for further treatment in a PC via a data acquisition system.

When the steady state is established (constant evaporator temperature), a fixed amount of water (four liters) is poured in the water tank that surrounds the evaporator, as shown in figure 5.

III.3. Data reduction

The cooling capacity $\dot{Q}_{CV}$ is estimated by calculating the heat exchanged between the evaporating refrigerant and the water causing its cooling and the decrease of its internal energy U_W

$$U_W = m_W C_{p,W} (T - T_{ref}) \tag{1}$$

$$\frac{dU_W}{dt} = m_W C_{p,W} \frac{dT}{dt} \tag{2}$$

Neglecting heat infiltration from outside the tank, the energy balance for the water writes:

$$\left(\frac{dU_W}{dt}\right) = \dot{Q}_{CV} \tag{3}$$

Hence,

$$\dot{Q}_{CV} = m_W C_{p,W} \frac{dT}{dt} \tag{4}$$

The coefficient of performance *COP* is calculated taking into account the heat loss from the generator.

$$COP = \frac{\dot{Q}_{CV}}{\dot{Q}_G - \dot{Q}_{loss}} \tag{5}$$

IV. Results and discussion

The performance of the system is investigated for various bubble pump heat inputs, from 170 W - the minimal heat power needed to start the machine - to 350 W. This heat input interval corresponds to a driving temperature ranging from 120 to 150°C.

IV.1 Effect of the heat input on the bubble pump temperature

Figure 6 shows the time evolution of the bubble pump temperature for different pump heat inputs. It can be noticed that for the lowest heat input, Q_{bp} = 170 W, the temperature increases progressively, reaches a maximum of 138°C after approximately 60 minutes, drops then sharply to 100°C and fluctuates thereafter periodically between these limits. The observed behavior confirms previous study results of bubble pump flow [7]. Each peak can be interpreted as the achievement of a pumping action: it represents the ejection of the solution into the separator. The temperature dropping is due to the entering of fresh solution in replacement of the pumped liquid.

The same figure shows also that the higher the heat flux is, the lower is the start-up time: when the heat input is increased from 170 to 350 W, the time elapsed to reach the first temperature peak (start-up of the pumping action) is reduced from 60 to 12 minutes. Furthermore, for higher heat fluxes the frequencies of the temperature oscillations are strongly increased and their amplitudes reduced, such that the temperature oscillations are progressively damped and finally vanish. An increasing frequency of temperature oscillations corresponds to increased pumping action caused by the higher added heat flux. From a bench heat input (Q_{bp} = 260 W) on, the temperature of the pumped liquid solution approaches that of the tube surface and the oscillations disappear.

IV.2 Effect of the heat input on different machine's operating temperatures

The time evolution of the temperature at different locations in the machine are monitored and observed. As illustration the temperatures of the vapor/liquid mixture in the bubble pump, the pumped solution, the vapor at the condenser inlet and in the evaporator for heat inputs to the bubble pump of respectively Q_{bp} = 170, 216 and 260 W are depicted in figures 7, 8 and 9.

One can observe (cf. Figs. 7 and 8) that the pumped solution temperature and that of the bubble pump are varying in concert: the pumped solution temperature starts decreasing synchronously when the bubble pump temperature begins dropping due to the refreshment of the tube's head by conduction (copper tube conductivity) and convection through the new solution arriving to the bubble pump. It can also be seen (Fig. 7) that the solution temperature gets further heated for 8-9 minutes more.

This time is strongly reduced when the heat input is increased to Q_{bp} = 216 W as shown in figure 8. The pumping action frequency is now higher. One can further notice on these same figures that the condenser inlet temperature is in phase opposition with the pump temperature. These figures reveal also that the evaporator temperature first remains constant starts dropping as soon as the bubble pump begins working. The temperature oscillations here are highly damped.

Figure 9 illustrates again the coupled evolution of the temperatures at different locations in the machine. Actually as soon as the bubble pump temperature oscillations disappear, the oscillations of all other temperatures disappear too.

IV.3 Effect of the heat input on the machine's performance

The cooling capacity and the *COP* are calculated for different heat inputs. Figure 10 shows the correlation between the cooling capacity, the *COP* and the tank water temperature for Q_{bp} = 260 W.

Figures 11 and 12 illustrate the variation of the cooling capacity and the *COP* of the machine with the heat input for T_{water} respectively of 9°C and 11°C. They show a strong dependency of the cooling capacity and the *COP* on the heat added to the bubble pump.

As expected, the variation of the cooling capacity and that of the *COP* confirm the results of reference [8].

According to figure 11, the cooling capacity and the *COP* rise simultaneously when the heat input is increased from 170 to 270 W. The increasing of the driving heat power leads to a higher cooling capacity until a maximum value is reached. Heating the solution in the generator beyond this limit is not necessary: the supplementary heat added is rejected as waste heat to the cooling air in the rectifier and the condenser. As a consequence, the *COP* beyond this limit gets lower.

The same behavior of the *COP* and the cooling capacity with heat power input is observed (Fig. 12) when the water is cooled to 11°C instead of 9°C in the preceding case. The maximum cooling capacity reaches now a maximum value of approximately 47 W.

The optimal *COP* is 0.175, corresponding to heat input of Q_{bp} = 265 W and a heat source temperature of near 140°C.

IV.4 Absorber temperature

Figure 13 depicts the time evolution of the rich solution temperature at the absorber outlet. It can be seen that this temperature is also sensitive to the heat input and, like the temperatures of other components of the machine, performs oscillations resulting from the working regime of the bubble pump. In fact, for Qbp = 170 W (start up power) the temperature increases from the ambient (20°C) to 48°C then oscillates periodically between 48 and 44°C (average 46°C). When the heat power input increases the oscillations are damped and disappear. For Qbp = 350W (the highest heat power) the temperature rises from ambient temperature to 48°C first then stabilizes approximately at 46°C. In any case the average temperature converges to this value whatever the heat input is.

The difference between the temperature of the exiting rich solution and that of the cooling air is the highest (25°C) at the bottom of the absorber, whilst it is of only 5°C at the top.

V. Conclusion

A low capacity (ca. 50 W) thermal driven diffusion absorption machine based on light hydrocarbons is designed, constructed and tested for various heat power inputs. The experimental results show that the bubble pump exiting temperature as well as those of the major components of the machine but the absorber is very sensitive to the heat power inputs to the bubble pump. For bubble pump heat inputs from 170 to 350 W, the driving temperature varies in the range 120-150°C. The lowest temperature reached at the evaporator entrance is -10°C provided by a driving temperature 138°C and a power inlet Q_{bp} = 260W. The *COP* of the machine has reached a maximum of 0.14 for T_{water} = 9°C and Q_{bp} = 275 W.

Acknowledgements

This work is part of a R&D project funded by the Spanish Ministry of Education and Science within the energy program ENE2006-15250.

It continues the investigations started in the R&D project "PRF Froid solaire (2003-2007)" funded by the Tunisian Ministry of Higher Education, Scientific Research and Technology.

References

1. B.C. Von Platen, C.G. Munters. US Patent 1, 685,764, 1928.
2. A. Koyfman, M. Jelinek, A. Levy, I. Borde, An experimental investigation of bubble pump performance for diffusion absorption refrigeration system with organic working fluids, Applied Thermal Engineering 23 (2003) 1881-1894.
3. Domestic © 2003, www.dometic.com (formerly known as Electrolux in Europe).
4. U. Jakob, U. Eicker, D. Schneider, A.H. Taki, M.J. Cook, Simulation and experimental investigation into diffusion absorption cooling machines for air conditioning applications, Applied Thermal Engineering (2007).
5. A. Zohar, M. Jelinek, A. Levy, I. Brode, Numerical investigation of a diffusion-absorption refrigeration cycle, Int. J. Refrigeration 28(4) (2005) 515–525.
6. A. Zohar, M. Jelinek, A. Levy, I. Brode, the influence of diffusion absorption refrigerant cycle configuration on the performance, Applied Thermal Engineering 27 (2007) 2213-2219.
7. R. Saravanan, M.P Maiya, Experimental analysis of a bubble pump operated H2O-LiBr vapour absorption cooler, Applied Thermal Engineering 23 (2003) 2383-2397.
8. J. Chen, K.J. Kim, K.E. Herold, Performance enhancement of a diffusion-absorption refrigerator, Int. J. Refrigeration 19 (3) (1996) 208-218.
9. N. Ben Ezzine, Kh. Mejbri, M. Barhoumi, A. Bellagi, Thermodynamic analysis and multi-parametric optimisation of double effect absorption chiller , International Journal of Exergy, Vol. 3, N°1, 2006, 68-86.

Figure captions

Figure 1. Diffusion absorption refrigerator working principle

Figure 2. Schematic assembly diagram of diffusion absorption machine

Figure 3. Condenser design

Figure 4. Absorber

Figure 5. Water tank around evaporator

Figure 6. Time evolution of the bubble pump temperature for various heat inputs

Figure 7. Variation of temperature for heat input Qbp = 170 W

Figure 8. Variation of temperature for heat input Q_{bp} = 216 W

Figure 9. Variation of temperature for heat input Qbp = 260 W

Figure 10. Cooling capacity, *COP* and tank water temperature for Q_{bp} = 260 W

Figure 11. Variation of the machine's performance vs. heat input (T_{water} = 9°C)

Figure 12. Variation of the machine's performance vs. heat input (T_{water} = 11°C)

Figure 13. Variation with time of the rich solution temperature at the absorber outlet (170 and 350 W)

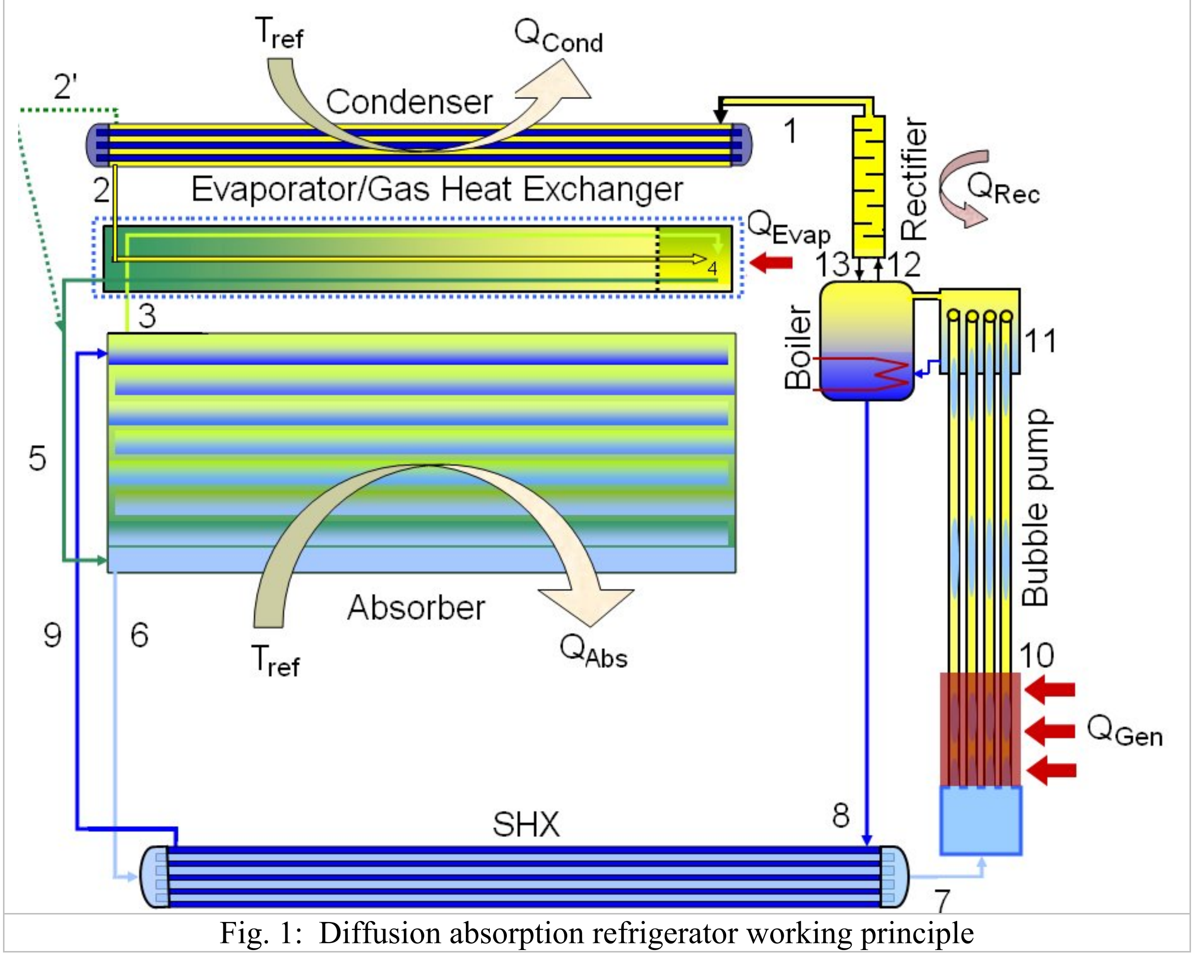

Fig. 1: Diffusion absorption refrigerator working principle

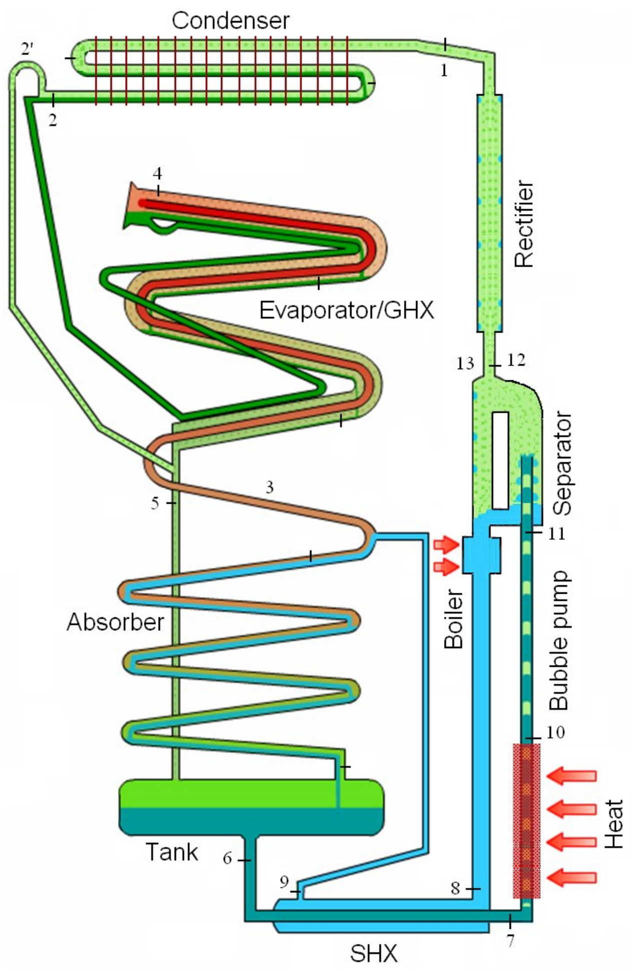

Fig. 2: Schematic assembly diagram of diffusion absorption machine

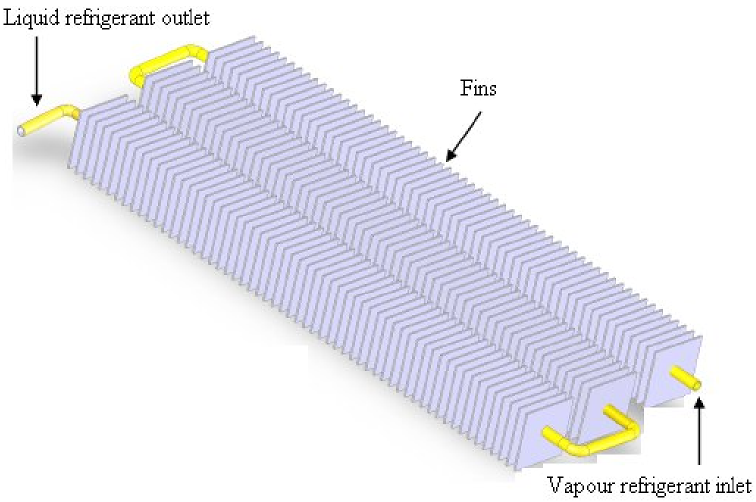

Fig. 3: Condenser design

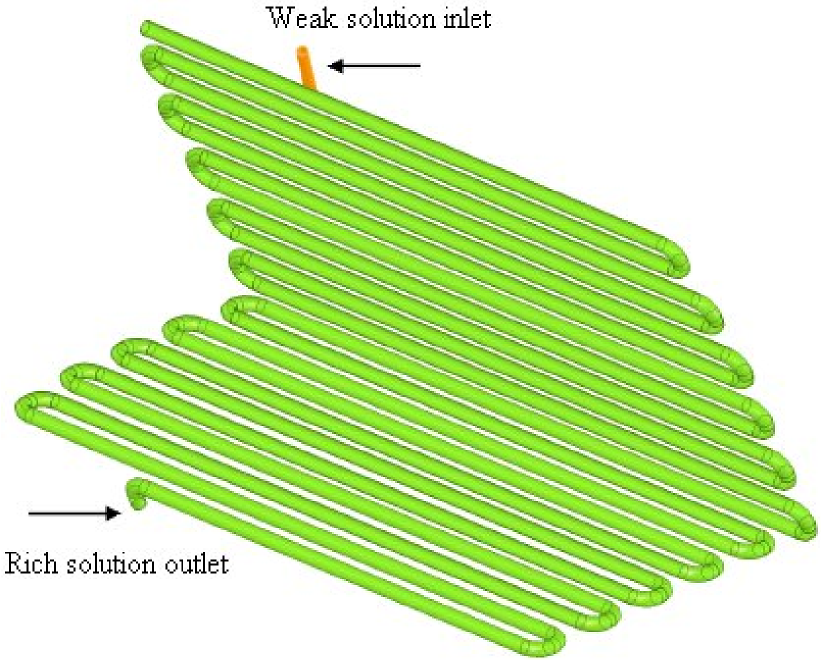

Fig. 3: Absorber

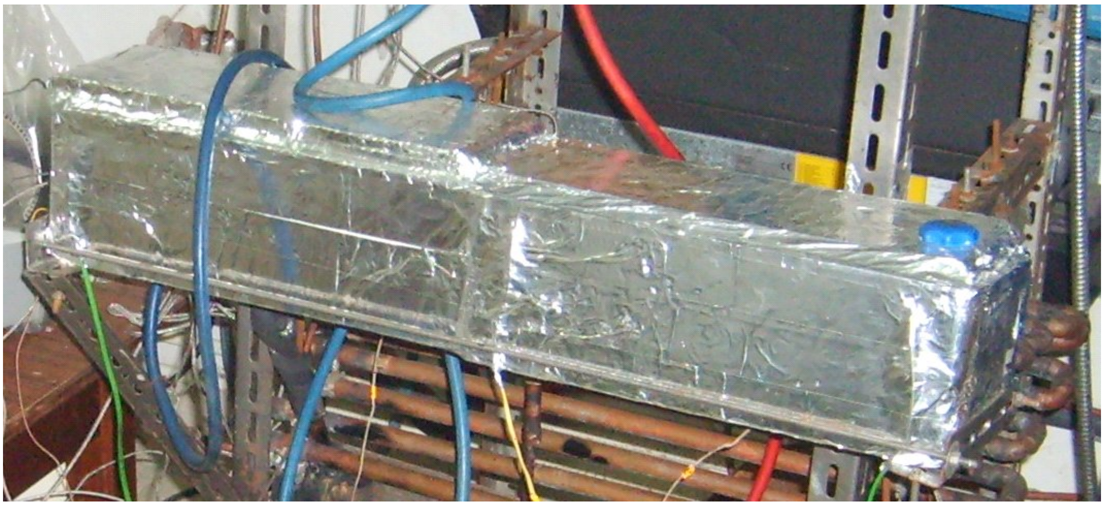

Fig. 5: Water tank around evaporator

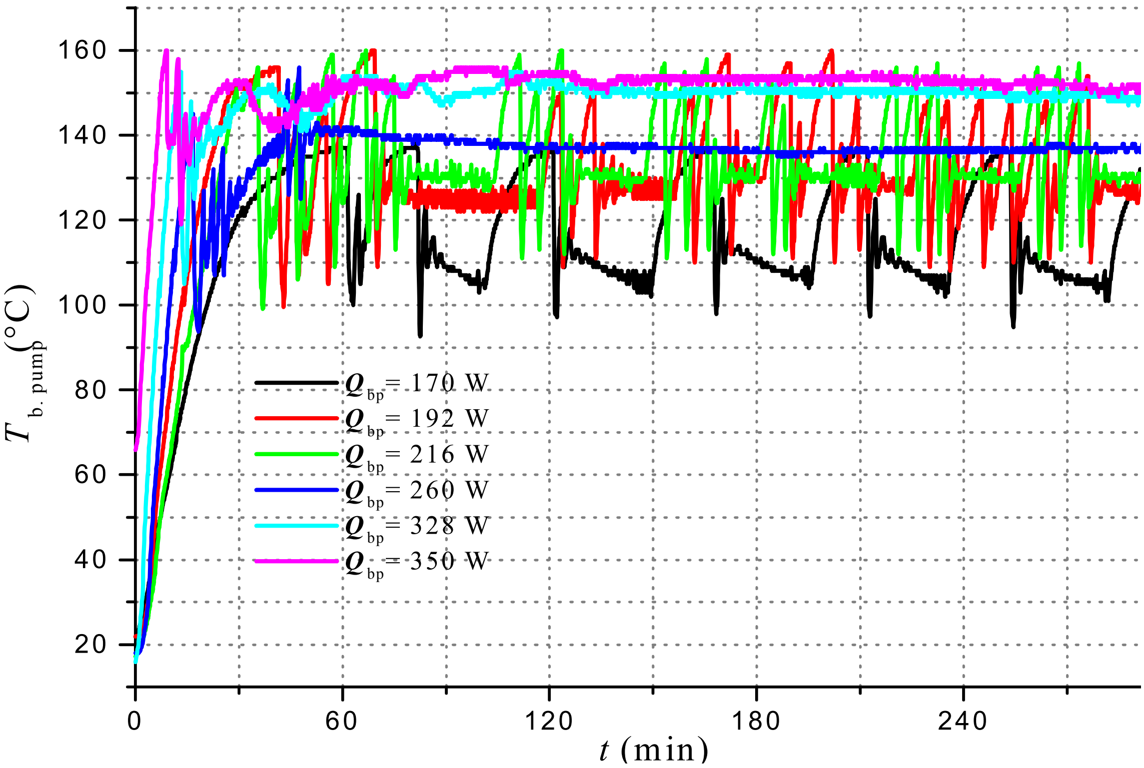

Fig. 6: Time evolution of the bubble pump temperature for various heat inputs

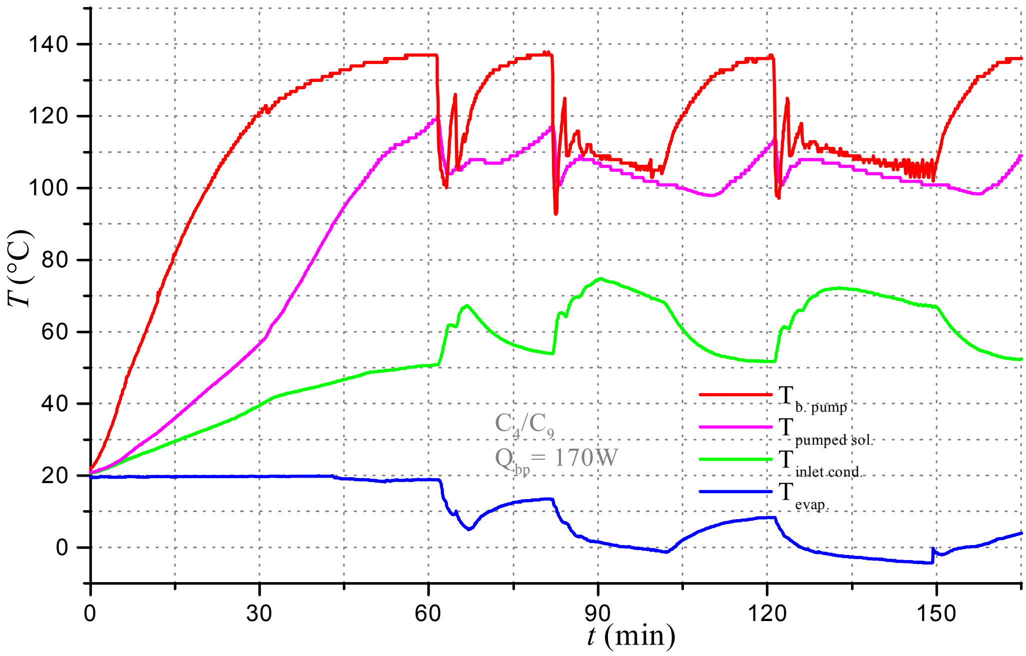

Fig. 7: Variation of temperature for heat input *Qbp* = 170 W

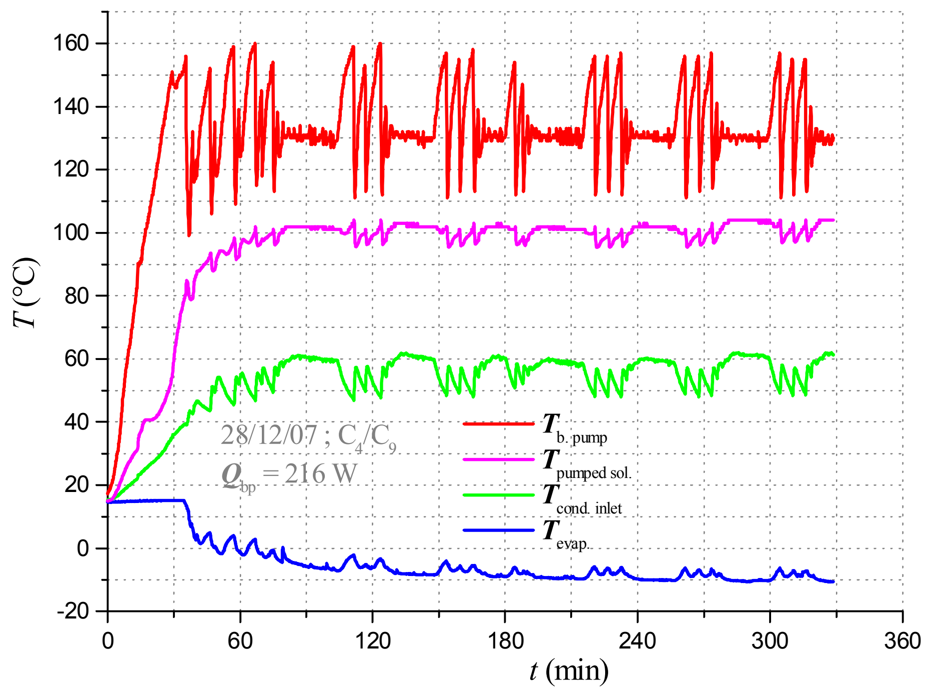

Fig. 8: Variation of temperature for heat input Q_{bp} = 216 W

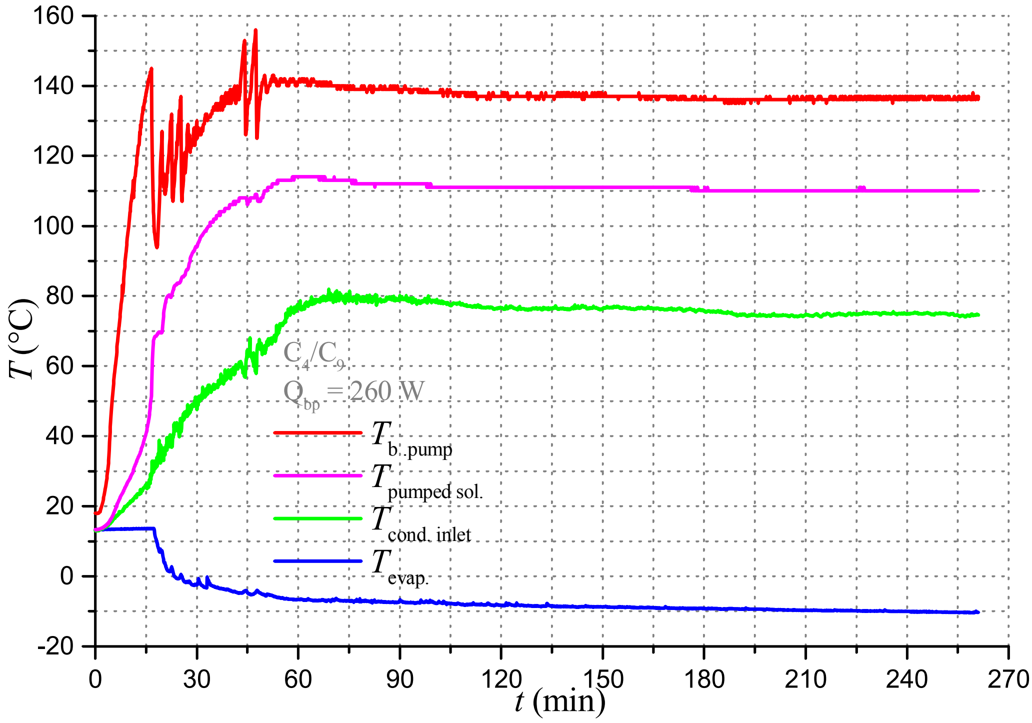

Fig. 9: Variation of temperature for heat input *Qbp* = 260 W

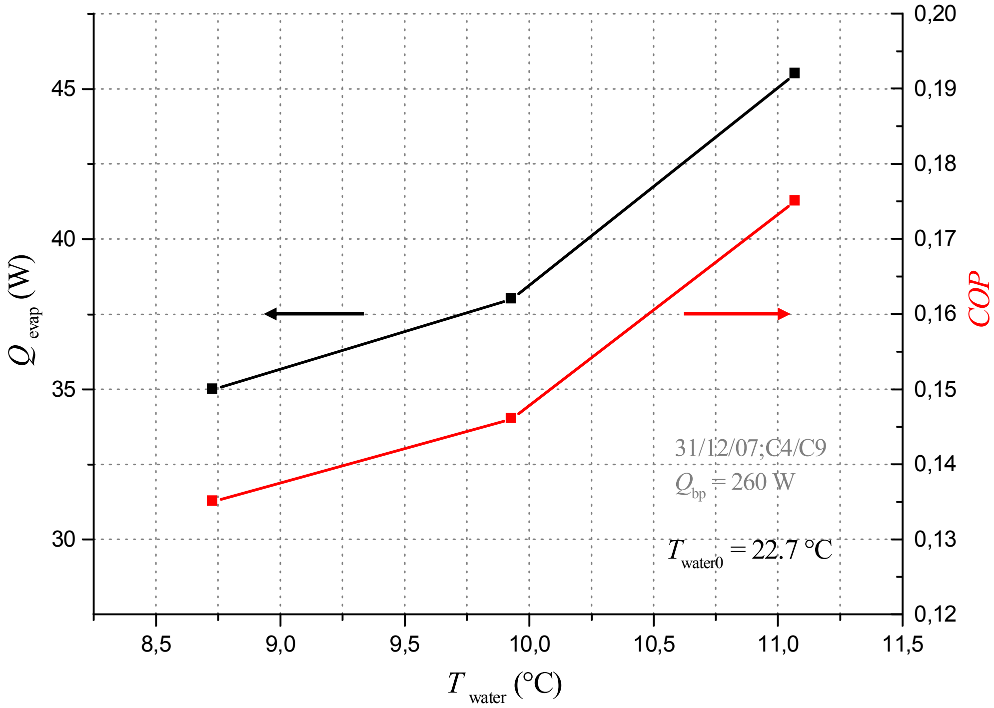

Fig. 10: Cooling capacity, *COP* and tank water temperature for Q_{bp} = 260 W

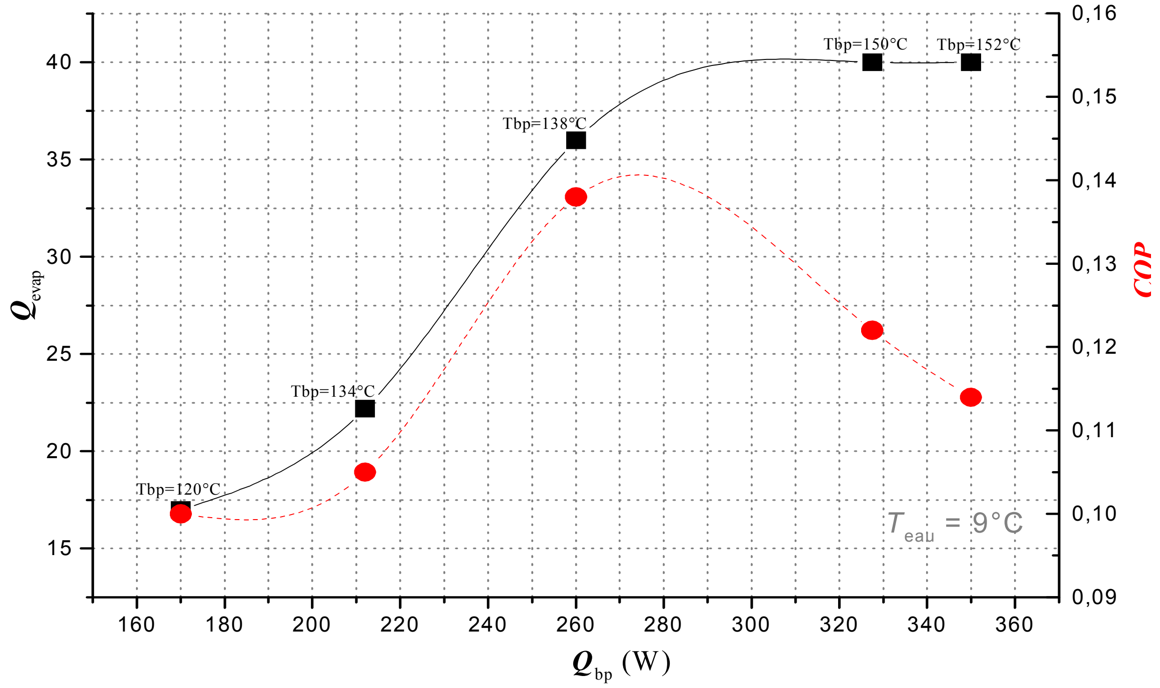

Fig. 11: Variation of the machine's performance *vs*. heat input (T_{water} = 9°C)

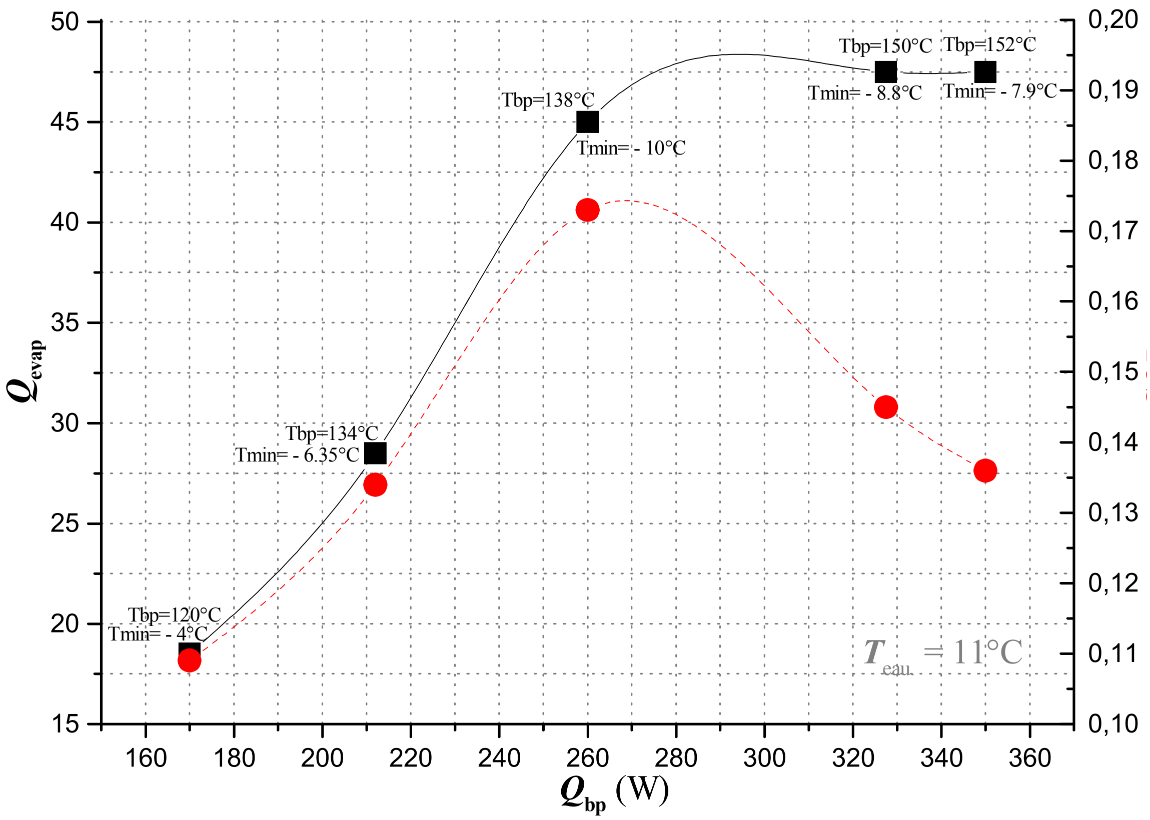

Fig. 12: Variation of the machine's performances vs. heat input (*Twater* = 11°C)

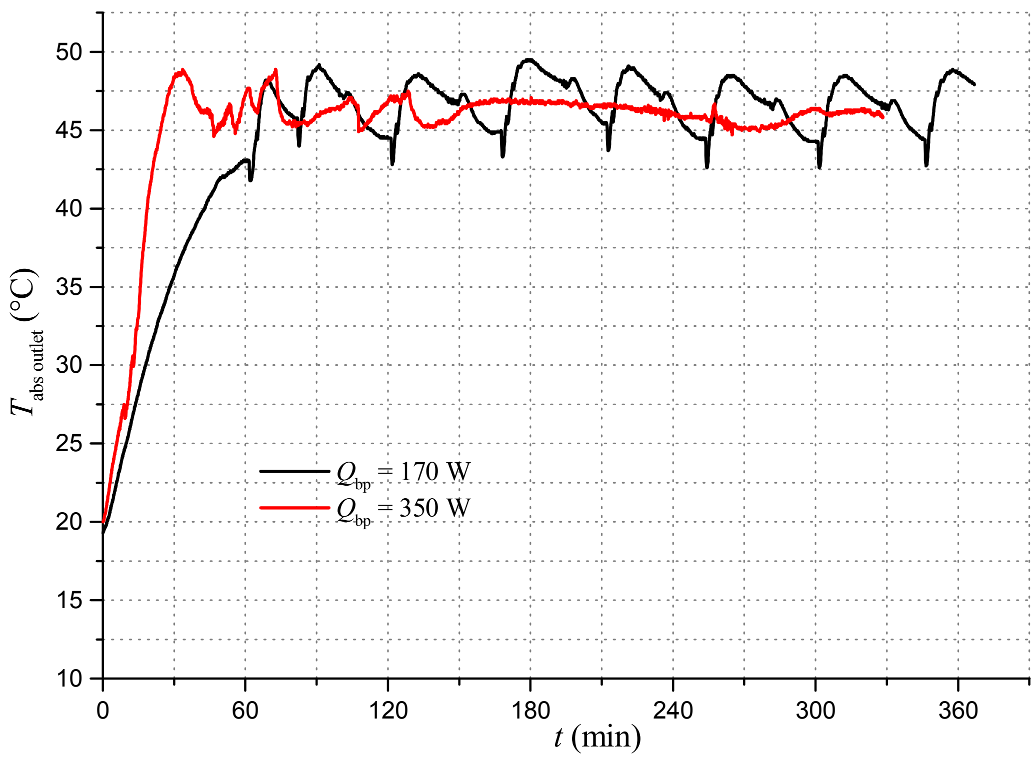

Fig. 13: Variation with time of the rich solution temperature at the absorber outlet

(170 and 350 W)